ChemComm

COMMUNICATION

Tailoring on-surface supramolecular architectures based on adenine directed self-assembly†

Cite this: *Chem. Commun.*, 2014, **50**, 356

Received 13th August 2013,
Accepted 25th October 2013

DOI: 10.1039/c3cc46149a

www.rsc.org/chemcomm

Qinggang Tan,‡[a] Chi Zhang,‡[a] Ning Wang,[a] Xiujuan Zhu,[b] Qiang Sun,[a] Mikkel F. Jacobsen,[c] Kurt V. Gothelf,[c] Flemming Besenbacher,[c] Aiguo Hu*[b] and Wei Xu*[ac]

From an interplay of high-resolution scanning tunneling microscopy (STM) imaging and density functional theory (DFT) calculations we demonstrate that by delicately choosing the parent molecule (adenine) we are able to tune the self-assembled nanostructures of adenine derivatives which are directed by the specific intermolecular interactions provided by the adenine moiety.

Controllable self-assembly of functional molecules has been a promising approach not only for constructing supramolecular nanostructures but also for realizing miniaturization and functionalization of molecule-based devices.[1–6] Employing certain templates, directing agents or external stimuli to precisely assemble molecules or nanoparticles in solution has proven to be an effective approach to fabricate desired functional nanostructures or nanodevices,[7–12] while directed arrangement of target moieties based on controllable on-surface self-assembly, yet, has attracted little attention to date. To explore such a process, one feasible route would be to take advantage of a well-studied parent molecule providing anticipated and reliable intermolecular interactions, and modify this parent molecule with a certain moiety at a specific position. With the templating effect provided by the parent molecule the target moiety could thus be arranged in a directed manner. Such a study may provide deeper insight into the role of the parent molecule in directing the formation of functional nanostructures especially with the possibility of extending to the third dimension, which could also shed light on the fabrication of on-surface molecular nanodevices.

In this communication, we present a detailed study of the directed self-assembly of two adenine derivatives (*p*-bromophenyl-modified adenine and *p*-bromobenzyl-modified adenine, shortened as BPA and BBA, respectively, as shown in Scheme 1a) on a Au(111) surface under ultrahigh vacuum conditions. Adenine, with the ability to form well-defined ribbon structures by intermolecular hydrogen bonding,[13–18] is chosen to be the parent molecule. It is seen that the BPA and BBA molecules are modified from adenine at a specific N9 site. We expect that such chemical modifications would not influence the potential hydrogen bonding for the formation of ribbon structures directed by the adenine moiety. From the interplay of high-resolution scanning tunneling microscopy (STM) imaging and van der Waals corrected density functional theory (vdW-DFT) calculations we show at the atomic-scale that the formation of well-ordered surface nanostructures

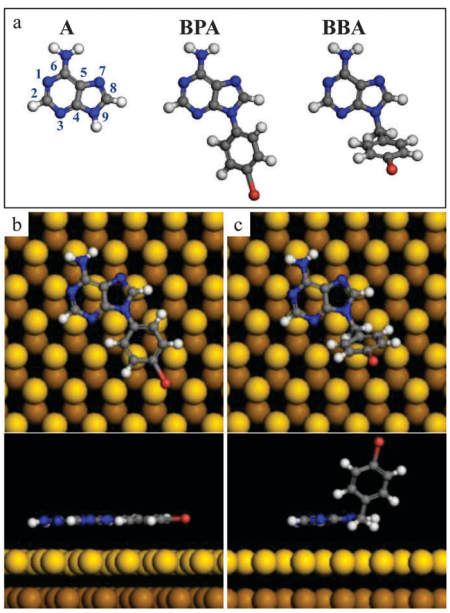

Scheme 1 (a) Gas-phase optimized structural models of adenine (A), *p*-bromophenyl-modified adenine (BPA) and *p*-bromobenzyl-modified adenine (BBA), respectively. (b) Top and side views of the DFT optimized structure of the BPA molecule adsorbed on a Au(111) surface. (c) Top and side views of the DFT optimized structure of the BBA molecule adsorbed on a Au(111) surface with the adenine moiety lying flat on the surface. Br: red, N: blue, C: gray, H: white, and Au: yellow.

[a] *College of Materials Science and Engineering, Key Laboratory for Advanced Civil Engineering Materials (Ministry of Education), Tongji University, Caoan Road 4800, Shanghai 201804, P. R. China. E-mail: xuwei@tongji.edu.cn*
[b] *School of Materials Science and Engineering, East China University of Science and Technology, Meilong Road 130, Shanghai 200237, P. R. China. E-mail: hagmhsn@ecust.edu.cn*
[c] *Interdisciplinary Nanoscience Center (iNANO), Department of Physics and Astronomy, Department of Chemistry, Aarhus University, 8000 Aarhus C, Denmark*

† Electronic supplementary information (ESI) available. See DOI: 10.1039/c3cc46149a

‡ These authors contributed equally.

of both BPA and BBA molecules is directed by the parent adenine moiety *via* double NH···N hydrogen bonds (*i.e.* employed in adenine ribbon structure), and moreover, the "joint" (*i.e.* methylene group) on the BBA molecule leads the bromophenyl moiety out of the surface plane which is also naturally regulated in the third dimension. These findings demonstrate the capability of arranging the moiety in 3D directed by the parent molecule, and open a way for aligning target moieties with increasing complexity and functions in the third dimension, which will be appealing for pursuit of more complicated 3D molecular nanodevices.

All the STM experiments were performed in a UHV chamber (base pressure 1×10^{-10} mbar) equipped with a variable-temperature "Aarhus-type" STM.[19,20] The Au(111) substrate was cleaned using a standard procedure. The BPA and BBA molecules were loaded in two separate glass crucibles in a molecular evaporator. After thoroughly degassing, we deposited the BPA and BBA molecules onto the clean Au(111) substrate held at room temperature, respectively, at ~370 K for a few minutes. The sample was thereafter transferred within the UHV chamber to the STM, where measurements were carried out over a temperature range of 120–150 K. All the calculations were performed by using the Vienna *ab initio* simulation package (VASP).[21,22] The projector augmented wave method was used to describe the interaction between ions and electrons.[23,24] We employed the PBE generalized gradient approximation exchange–correlation functional,[25] and van der Waals (vdW) interactions were included using the dispersion corrected DFT-D2 method of Grimme.[26] The atomic structures were relaxed using the conjugate gradient algorithm scheme as implemented in VASP until the forces on all unconstrained atoms were $\leq$0.03 eV Å^{-1}. The simulated STM images were obtained using the Tersoff–Hamann method.[27]

Upon deposition of BPA molecules on the Au(111) surface, a well-ordered self-assembled nanostructure is observed as shown in Fig. 1a. A closer inspection reveals that the single molecule appears as a dark triangle with a bright long oval. From the DFT optimized structure of the BPA molecule adsorbed on a Au(111) surface (*cf.* Scheme 1b), we can see that both the adenine moiety and the bromophenyl part tend to adopt flat-lying geometries on the surface. The typical STM image (*cf.* Fig. 1a) shows that the self-assembled nanostructure with an alternating zipper-like arrangement of the triangle parts resembles very much the adenine ribbon structure.[13–18] To further investigate the intermolecular interactions and the resulting self-assembled nanostructure, DFT calculations and STM image simulation (*cf.* Fig. S1, ESI†) have been performed. Fig. 1b shows the energetically most favorable gas-phase structural model with the binding energy of 0.71 eV per molecule, which is identified to be in good agreement with the experimental data. Combination of experimental and theoretical data suggests that the dark triangle and the bright long oval are attributed to the flat-lying adenine moiety and the bromophenyl part (the Br atom has higher contrast in the STM image), respectively. The white dashed lines in Fig. 1a and b show the correlation between the experimental and theoretical data and the in-between structure is the so-called adenine ribbon structure stabilized by Watson–Crick and Hoogsteen hydrogen bonds,[13,14] *i.e.* each BPA molecule links to the neighboring ones *via* two NH···N hydrogen bonds (indicated by the blue dashed lines) provided by the adenine moiety. The ribbons are subsequently linked together by weak CH···Br hydrogen bonds forming a zipper-like arrangement as well. To further recognize the dominant interaction directing the self-assembly process within the observed nanostructure, the charge density difference map is plotted as shown in Fig. 1c. Notable charge redistributions mainly gather around the double hydrogen bonds provided by the adenine moiety while the charge transfer of the weak CH···Br hydrogen bonds can only be visible when the isosurface value is at a rather small level indicating that the self-assembled nanostructure is predominantly directed by the adenine moiety through intermolecular hydrogen bonding.

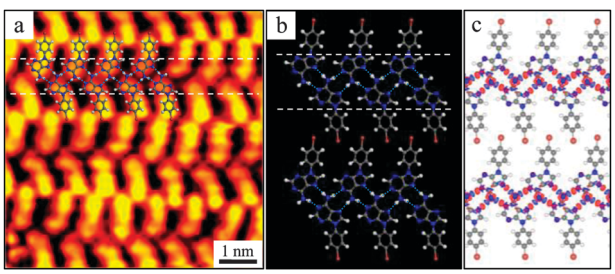

Fig. 1 (a) High-resolution STM image of self-assembled surface nanostructures formed by the BPA molecule superimposed with the DFT optimized ribbon structure. Scanning conditions: I_t = 0.5 nA, V_t = 1051 mV. (b) The DFT optimized structural model of the network structure. The white dashed lines both in (a) and (b) indicate the ribbon structures directed by the adenine moieties *via* double NH···N hydrogen bonds (*cf.* the blue dashed lines). (c) The corresponding charge density difference map of the nanostructure calculated at the isosurface value of 0.016 e Å^{-3}. Blue and red isosurfaces indicate charge depletion and accumulation, respectively.

Interestingly, different stripe structures are observed when the methylene group is added to connect the adenine moiety with the bromophenyl part (*cf.* BBA molecule in Scheme 1a), which increases the flexibility of the molecule on one hand and extends the molecule to the third dimension on the other hand. Combination of DFT calculations (*cf.* Fig. S2, ESI†) and STM images indicates that the BBA molecule would tend to adopt a non-planar adsorption geometry with the adenine moiety lying flat on the surface and the bromophenyl part out of the surface (*cf.* Scheme 1c). Deposition of BBA molecules on the Au(111) surface results in the formation of subtly different self-assembled nanostructures simultaneously and the representative STM images are shown in Fig. 2a and b. In both domains alternating zipper-like stripe structures are formed through the dark parts which are naturally assigned to the adenine moieties as the separations have been measured to be similar for structures shown in Fig. 1a, 2a and b (*cf.* Fig. S3, ESI†), while the bright ovals (the bromophenyl parts) tend to be, however, arranged in a face-to-face manner. To further investigate the intermolecular interactions and the resulting self-assembled nanostructure, DFT calculations and STM image simulations (*cf.* Fig. S4 and S5, ESI†) have been performed and the energetically most favorable gas-phase structural models of adenine-ribbon directed stripe structures are superimposed on the corresponding STM images as shown in Fig. 2c and d, respectively, where a good agreement is achieved. Moreover, line profiles across the whole molecule of BPA and BBA in the corresponding self-assembled structures (*cf.* Fig. S6, ESI†) are also compatible with the gas-phase structural models. From the comparison of experimental data and calculations we can identify that the difference in the two stripe structures lies in the chirality of the adenine moieties. The stripe structures in Fig. 2c and d are directed by the homochiral adenine ribbon and the heterochiral one, respectively. As a

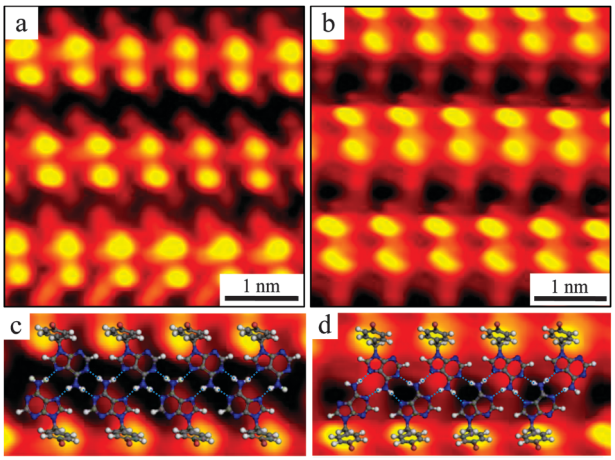

Fig. 2 (a) and (b) show high-resolution STM images of self-assembled surface nanostructures formed by the BBA molecule with the adenine ribbon structures being homochiral and heterochiral, respectively. Scanning conditions: I_t = 0.5 nA, V_t = 1051 mV. (c) and (d) show the corresponding close-up STM images superimposed with the DFT optimized structural models.

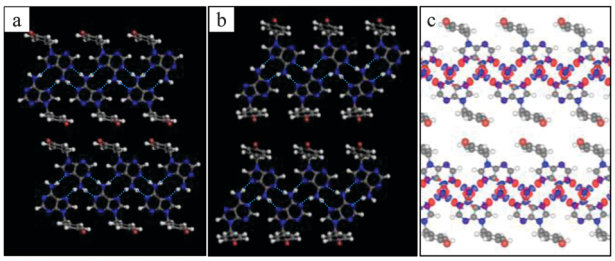

Fig. 3 (a) and (b) show the DFT optimized structural models of the network structures formed by the BBA molecule where the adenine ribbon is homochiral and heterochiral, respectively. (c) The charge density difference map of structure in (a) calculated at the isosurface value of 0.016 e Å^{-3}. Blue and red isosurfaces indicate charge depletion and accumulation, respectively.

consequence of the sp^3 hybridization of the connecting methylene group, the bromophenyl part in the BBA molecule is significantly tilted from the flat-lying adenine moiety which leads to the increased apparent height in STM images.

To gain further insight into the interactions between the neighboring stripes, we also performed a wide structural search by proposing several possible structures from the gas-phase calculations and obtained the energetically most favorable network structures with the binding energy of 0.78 eV per molecule and 0.68 eV per molecule as shown in Fig. 3a and b, respectively. The tilted bromophenyl parts interact with the neighboring ones by van der Waals interactions in a face-to-face manner. Considering the similarity of the two network structures, only the charge density difference map of the nanostructure of Fig. 3a is plotted as shown in Fig. 3c. As illustrated from the charge density difference map, the main charge transfers also concentrate on double NH$\cdots$N hydrogen bonds indicating the dominant interaction, which is in analogy to the nanostructure formed by the BPA molecule. These observations together with the calculations validate that the double hydrogen bonds provided by the adenine moiety are capable of directing the self-assembled process as expected, while the secondary weak CH$\cdots$Br hydrogen bonds or van der Waals interactions further stabilize the adenine-directed ribbon structures in the whole network.

In conclusion, from an interplay of high-resolution STM imaging and DFT calculations, we have investigated the directed self-assembly of two adenine derivatives on the Au(111) surface and presented the influence of different modified groups on the resulting self-assembled patterns. Our results demonstrate that by delicately choosing the parent molecule we are able to tune the self-assembled nanostructures directed by the specific intermolecular interactions provided by the parent molecule. Such kind of directed self-assembly may provide an interesting and simple route for building desired nanostructures even extending to the third dimension, which would be interesting for design and fabrication of functional nanodevices using the bottom-up strategy.

The authors acknowledge the financial support from the National Natural Science Foundation of China (21103128, 91023008), the Shanghai Pujiang Program (11PJ1409700), the Shanghai "Shu Guang" Project supported by Shanghai Municipal Education Commission and Shanghai Education Development Foundation (11SG25), the Fundamental Research Funds for the Central Universities, the Research Fund for the Doctoral Program of Higher Education of China (20120072110045), and the Shanghai Leading Academic Discipline Project (B502).

Notes and references

1 K. S. Mali, J. Adisoejoso, E. Ghijsens, I. De Cat and S. De Feyter, *Acc. Chem. Res.*, 2012, **45**, 1309.
2 S. S. Li, H. J. Yan, L. J. Wan, H. B. Yang, B. H. Northrop and P. J. Stang, *J. Am. Chem. Soc.*, 2007, **129**, 9268.
3 S. De Feyter and F. C. De Schryver, *Chem. Soc. Rev.*, 2003, **32**, 139.
4 J. A. Theobald, N. S. Oxtoby, M. A. Phillips, N. R. Champness and P. H. Beton, *Nature*, 2003, **424**, 1029.
5 J. A. Elemans, R. van Hameren, R. J. Nolte and A. E. Rowan, *Adv. Mater.*, 2006, **18**, 1251.
6 T. Yokoyama, S. Yokoyama, T. Kamikado, Y. Okuno and S. Mashiko, *Nature*, 2001, **413**, 619.
7 W. Shenton, S. A. Davis and S. Mann, *Adv. Mater.*, 1999, **11**, 449.
8 C. J. Loweth, W. B. Caldwell, X. Peng, A. P. Alivisatos and P. G. Schultz, *Angew. Chem., Int. Ed.*, 1999, **38**, 1808.
9 Q. Chen, S. C. Bae and S. Granick, *Nature*, 2011, **469**, 381.
10 A. Kuzyk, R. Schreiber, Z. Fan, G. Pardatscher, E. M. Roller, A. Högele, F. C. Simmel, A. O. Govorov and T. Liedl, *Nature*, 2012, **483**, 311.
11 L. Zheng, X. Qiu, Y. Xu, J. Fu, Y. Yuan, D. Zhu and S. Chen, *CrystEngComm*, 2011, **13**, 2714.
12 M. Grzelczak, J. Vermant, E. M. Furst and L. M. Liz-Marzán, *ACS Nano*, 2010, **4**, 3591.
13 D. Dobrzynska and L. B. Jerzykiewicz, *J. Am. Chem. Soc.*, 2004, **126**, 11118.
14 W. Zierkiewicz, D. Michalska and P. Hobza, *Phys. Chem. Chem. Phys.*, 2010, **12**, 2888.
15 R. E. A. Kelly, W. Xu, M. Lukas, R. Otero, M. Mura, Y. J. Lee, E. Lægsgaard, I. Stensgaard, L. N. Kantorovich and F. Besenbacher, *Small*, 2008, **4**, 1494.
16 L. M. Perdigão, P. A. Staniec, N. R. Champness, R. E. A. Kelly, L. N. Kantorovich and P. H. Beton, *Phys. Rev. B*, 2006, **73**, 195423.
17 M. Lukas, R. E. A. Kelly, L. N. Kantorovich, R. Otero, W. Xu, E. Laegsgaard, I. Stensgaard and F. Besenbacher, *J. Chem. Phys.*, 2009, **130**, 024705.
18 M. J. Capitán, R. Otero, J. Álvarez and R. Miranda, *ChemPhysChem*, 2011, **12**, 1267.
19 F. Besenbacher, *Rep. Prog. Phys.*, 1996, **59**, 1737.
20 E. Lægsgaard, L. Österlund, P. Thostrup, P. B. Rasmussen, I. Stensgaard and F. Besenbacher, *Rev. Sci. Instrum.*, 2001, **72**, 3537.
21 G. Kresse and J. Hafner, *Phys. Rev. B*, 1993, **48**, 13115.
22 G. Kresse and J. Furthmüller, *Phys. Rev. B*, 1996, **54**, 11169.
23 P. E. Blöchl, *Phys. Rev. B*, 1994, **50**, 17953.
24 G. Kresse and D. Joubert, *Phys. Rev. B*, 1999, **59**, 1758.
25 J. P. Perdew, K. Burke and M. Ernzerhof, *Phys. Rev. Lett.*, 1996, **77**, 3865.
26 S. J. Grimme, *Comput. Chem.*, 2006, **27**, 1787.
27 J. Tersoff and D. R. Hamann, *Phys. Rev. B*, 1985, **41**, 805.